

See discussions, stats, and author profiles for this publication at: <https://www.researchgate.net/publication/272295663>

Ionic Liquid Cross-Linked Multifunctional Cationic Polymer Nanobeads via Dispersion Polymerization: Applications in Anion Exchange, Templates for Palladium, and Fluorescent Carbon...

ARTICLE *in* THE JOURNAL OF PHYSICAL CHEMISTRY C · FEBRUARY 2015

Impact Factor: 4.77 · DOI: 10.1021/jp510804x

CITATIONS

2

READS

84

4 AUTHORS, INCLUDING:



Tamalika Das

University of Calcutta

9 PUBLICATIONS 5 CITATIONS

[SEE PROFILE](#)



Mrinmoy Biswas

Indian Association for the Cultivation of Science

11 PUBLICATIONS 59 CITATIONS

[SEE PROFILE](#)



Tarun Mandal

Indian Association for the Cultivation of Science

82 PUBLICATIONS 2,325 CITATIONS

[SEE PROFILE](#)

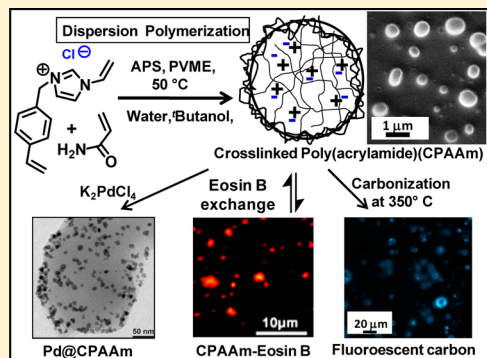
Ionic Liquid Cross-Linked Multifunctional Cationic Polymer Nanobeads via Dispersion Polymerization: Applications in Anion Exchange, Templates for Palladium, and Fluorescent Carbon Nanoparticles

Tamalika Das, Tapas K. Paira, Mrinmoy Biswas, and Tarun K. Mandal*

Polymer Science Unit, Indian Association for the Cultivation of Science, Jadavpur, Kolkata 700 032, India

S Supporting Information

ABSTRACT: This report describes the design and synthesis of an ionic liquid by simple nucleophilic substitution reaction of 4-vinylbenzyl chloride and *N*-vinylimidazole. This ionic liquid is utilized as cross-linker for dispersion polymerization of acrylamide in the presence of poly(vinyl methyl ether) (PVME) stabilizer, which produces water-friendly cationic cross-linked poly(acrylamide) (CPAAm) beads. Morphology investigation reveals that these beads are nanosized and spherical and their size varies with the amount of cross-linker and PVME used. The ionic cross-linker imparts ionic nature in these beads, where anion is mobile and are eventually exchangeable. Consequently, anion exchange capacity is checked using an anionic dye Eosin B via UV-vis spectroscopy. Subsequently, the release of dye is monitored on addition of a pinch of sodium acetate. Analogous anion exchange with $[PdCl_4]^{2-}$ results in the formation of palladium (Pd) nanoparticles (NPs) inside the cross-linked poly(acrylamide) beads due to *in situ* reduction by imidazolium cation present in CPAAm. The carbonization of the CPAAm nanobeads produces nitrogen-doped carbon nanoparticles of comparable morphology and sizes. The resultant carbon nanoparticles emit blue fluorescence under irradiation of UV light. Similarly, Pd NPs embedded carbon nanoparticles are easily prepared by carbonization of the Pd NPs loaded CPAAm nanobeads.



INTRODUCTION

Polymeric nanospheres have attracted much attention due to their broad range applications in drug delivery,^{1,2} chromatography,^{3,4} biochemical supports,⁵ catalysis,⁶ paints and coatings,⁷ etc. Dispersion polymerization is in principle a very attractive and most extensively used method to prepare monodisperse polymeric particles in the size range of 1–10 μm in a single step, which involves monomer, initiator, and a surface stabilizer in a particular dispersion medium.⁸ Thus, the dispersion polymerization technique has been widely used for preparing nano/microspheres of various polymers.^{8–11} This polymerization technique has also been used for making cross-linked polymeric bead.^{11–13} However, the reports of preparing nanostructured cross-linked poly(acrylamide) (CPAAm) beads are less, which can be prepared using acrylamide as monomer and methylenebis(acrylamide) as cross-linker along with a stabilizer showing stable dispersion in water, as poly(acrylamide) (PAAm) is a water-friendly polymer.¹⁴ On the other hand, ionic liquids have recently received keen interest from academia due to its good thermal stability, electrical conductivity, polarity, and tunable solubility.^{15,16} However, the use of ionic liquid as a cross-linker is a rare phenomenon in dispersion polymerization, which is expected to introduce electrostatic charge into the CPAAm beads and thereby make it useful as ion exchange material.^{17–19} So far, ionic monomer

serves the purpose of preparing ionic polymeric beads capable of ion exchange. Whereas, the use of ionic liquid cross-linker would disclose the possibility of tuning the ionic nature of the polymer bead.^{14,20}

It is known that ionic liquids (ILs) and poly(ionic liquid)s are self-assembled in solution and can act as soft template to generate metal nanoparticles.^{21–25} In many occasions, ILs are suitably designed which not only tune the morphology but also act as reductant to generate metal nanoparticle (NP) from metal salts as reported by our group in synthesizing different anisotropic shaped gold nanoparticles.²³ In another work, Precht and his group synthesized stable ruthenium and nickel nanoparticles in the absence of classical reducing agent in imidazolium ionic liquid.²⁴ Thiot with his team developed a method for preparing palladium (Pd) nanoparticles (NPs) using poly(ionic) gels of a Merrifield type resin.²⁵ However, there are few reports of designing of new ILs or PILs that can act as a precursor, reducing agent, and template all together.

Carbon nanoparticle had been in the limelight for the past two decades owing to their exponentially increasing applications in the diversified domains of electronics,²⁶ water

Received: October 28, 2014

Revised: January 29, 2015

Published: February 2, 2015

purification,^{27–30} heterogeneous catalysis,^{31–34} chemical sensing,³⁵ energy, and hydrogen storage even in harsh environments of applied fields.^{36,37} The major reasons for their attraction in the application fields arise from their remarkable properties like high surface area, chemical inertness, good conductivity, and stability.^{34,38} Several different synthetic strategies using inorganic hard template like zeolite sieves,^{39–41} silica gel,⁴² mesoporous silica,^{43–48} silica nanoparticles,^{49–52} magnesium oxide,⁵³ and zinc oxide⁵⁴ have been adopted to develop highly ordered mesoporous carbon (MC) materials with narrow pore size distribution. However, the major disadvantage of the above methodology is the elaborate template removal process which also requires hazardous chemicals like HF. Self-assembled block copolymer based soft micelle templating is an alternative technique^{55–58} but generally overlooked due to thermal instability to produce rigid carbon nanostructure.⁵⁹ However, carbon nanoparticles have never been synthesized directly from any cross-linked polymer beads, where covalent interconnection imparts rigidity and need no additional template removal step. Recently, a new generation of organic material belonging to ionic liquids or poly(ionic liquid)s have been extensively used to synthesize carbon nanostructures, which ensures nitrogen doping and higher dispersity in polar solvent.^{15,16}

Herein, we report the synthesis of nanostructured cross-linked cationic poly(acrylamide) (CPAAM) beads by dispersion polymerization using a designed vinylimidazolium-based ionic liquid as cross-linker and poly(vinyl methyl ether) (PVME) as surface stabilizer. The formed polymeric beads are well-dispersed in water. The morphology and size of the beads depend on the relative amount of cross-linker and surface stabilizing polymer used. The change of the ionic potential with the variation of the amount of cross-linker is also investigated. Ion exchange of cationic CPAAM beads are successfully performed using an anionic dye Eosin B. Additionally, using sodium acetate, the release of the dye is checked which justify its use as a specific anionic dye vehicle. Similarly anion exchange is also performed using $[PdCl_4]^{2-}$ ion to prepare ionic liquid cross-linked PAAm precursor beads for generation of palladium nanoparticles (Pd NPs). Surprisingly, Pd NPs are *in situ* produced inside the polymer cage without any the use of conventional reducing agent. The CPAAM beads are also employed to prepare nitrogen-doped carbon nanoparticles (NC NPs) by anaerobic carbonization. This method generates stable NC NPs by replicating the CPAAM beads, which exhibits strong blue fluorescence under UV light. Similarly, nitrogen-doped carbon palladium conjugate nanostructures is also prepared from the above-mentioned Pd embedded CPAAM (Pd@CPAAM) conjugate.

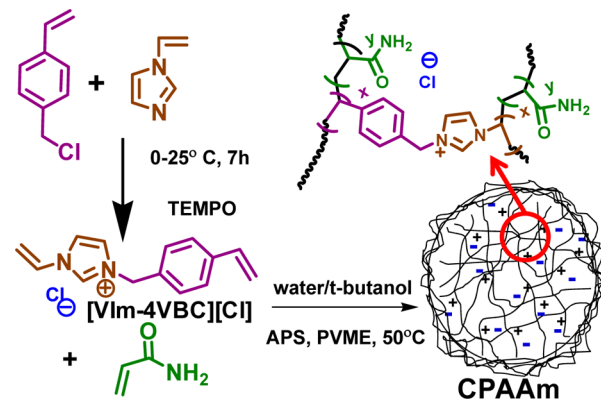
EXPERIMENTAL DETAILS

Materials. 4-Vinylbenzyl chloride (4VBC), (2,2,6,6-tetramethylpiperidin-1-yl)oxyl [TEMPO], tetramethylethylenediamine (TEMED), and potassium tetracholopalladate(II) (K_2PdCl_4) were purchased from Aldrich and were used as received. N-Vinylimidazole (VIm) was received from Aldrich and purified by vacuum distillation prior to use. Acrylamide (AAm), ammonium persulfate (APS), and *tert*-butanol were purchased from Merck, India. Monomer acrylamide was recrystallized from hot chloroform. Initiator APS was also recrystallized from lukewarm water. *tert*-Butanol was distilled over CaH_2 just before use. Poly(vinyl methyl ether) (PVME) (MW = 52 000) was obtained from Aldrich, as 50 wt %

aqueous solution, which was heated to 50 °C to precipitate out. The supernatant was discarded, and the residual solid PVME was dried at 70 °C in a vacuum for 1 h before use. Eosin B and Crystal violet were bought from Merck, Germany. Milli-Q water was used during polymerization and in preparation of various aqueous solutions.

Synthesis of an Ionic Liquid Cross-Linker [VIm-4VBC][Cl]. A new ionic liquid based cross-linker, [VIm-4VBC][Cl], was synthesized by nucleophilic substitution reaction between *N*-vinylimidazole (VIm) and 4-vinylbenzyl chloride (4VBC) (1:1 molar ratio) at room temperature as shown in Scheme 1. *N*-Vinylimidazole was first mixed with

Scheme 1. Schematic Representation for the Synthesis of Ionic Liquid Cross-Linker, [VIm-4VBC][Cl], and Its Use in the Dispersion Polymerization of Acrylamide To Prepare Cross-Linked Poly(acrylamide) (CPAAM) Beads



catalytic amount of TEMPO (radical quenchers), and the reaction mixture was cooled to 0 °C to add 4-vinylbenzyl chloride. Finally, the reaction mixture was kept at room temperature for 7 h. After completion of the reaction, the mass was dissolved in methanol partially, from which the ionic liquid product was precipitated in excess ethyl acetate. The prepared ionic liquid cross-linker was highly reactive and tends to self-polymerize; thus, it was stored under an argon atmosphere in a refrigerator. Further, as-prepared [VIm-4VBC][Cl] was characterized by ESI mass spectrometry and 1H NMR.

Preparation of Cross-Linked Cationic Poly(acrylamide) (CPAAM) Beads by Dispersion Polymerization of Acrylamide and [VIm-4VBC][Cl] Cross-Linker. The adopted polymerization method was a modified approach of Ray et al.⁶⁰ Typically measured amount of [VIm-4VBC][Cl] (0.02 g) was dissolved in 5 mL of aqueous solution of PVME (2 wt %) through continuous stirring in a long-neck 50 mL round-bottom flask. Acrylamide monomer (0.4 g), 5 mL of *tert*-butanol, and APS (0.025g) were successively added to the homogeneous solution under a N_2 atmosphere. Afterward, the mixture was warmed at 50 °C for 24 h. The entire dispersion polymerization process is represented in Scheme 1. Subsequently, we varied the concentration of the cross-linker, [VIm-4VBC][Cl], and stabilizer (PVME), keeping all other reaction parameters constant (see Table 1). Finally, the resultant polymer beads were purified through precipitation followed by centrifugation in acetone to remove excess PVME and other components. Finally, the precipitate was dried in a vacuum and powdered for subsequent studies.

Procedure for Eosin B Exchange and Release by Cationic CPAAM Beads. Aqueous solution of Eosin B, an

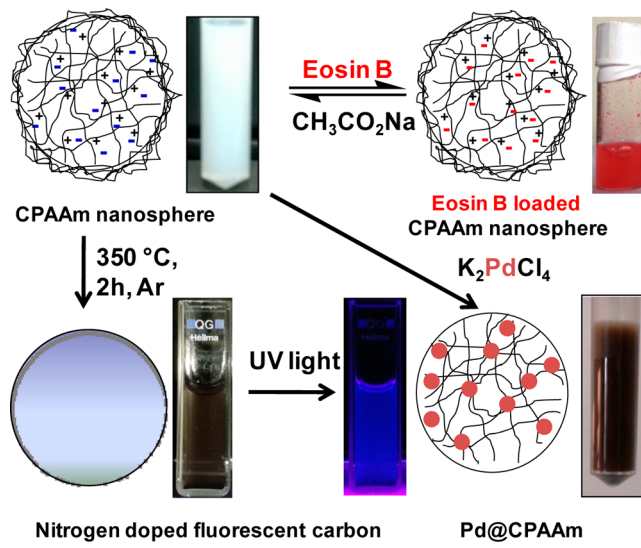
Table 1. Reaction Recipe for the Preparation of CPAAm Beads and Their Characterization

sample	monomer	% [VIm-4VBC] ⁺ Cl ⁻ ^a	wt % of PVME	D _{SEM} ^b (nm)	D _{DLS} ^c (nm)
CPAAM1	acrylamide (4 wt %)	5.0	1.0	480	714
CPAAM2		5.0	2.0	286	532
CPAAM3		5.0	4.0	242	295
CPAAM4		2.5	2.0	336	536
CPAAM5		10.0	2.0	147	300

^aMol % of ionic liquid cross-linker with respect to monomer. ^bD_{SEM}: diameter measured from the FESEM image. ^cD_{DLS}: hydrodynamic diameter measured by DLS.

anionic dye (2 mL, 10⁻⁵ M), was added to ~2 mg of the as-synthesized CPAAm beads and incubated for 24 h. The gradual uptake of the anionic dye with time by cationic CPAAm beads was monitored by recording a gradual decrease in absorbance of Eosin B in the supernatant solution after centrifugation of the dispersion of CPAAm. After 24 h, the CPAAm beads were repeatedly centrifuged to remove physically adsorbed dye for fluorescent spectroscopy and microscopy measurements. The dye release study involved incubation of aqueous dispersion of dye-loaded CPAAm beads in sodium acetate solution and succeeding recording of UV-vis absorbance of the supernatant, as described above. The dye uptake and release study was schematically represented in Scheme 2. A similar test was also performed with a cationic dye, crystal violet.

Scheme 2. Schematic Representation of the Different Application of Ionic CPAAm Nanospheres in Anion Exchange, Preparation of Pd NPs Embedded CPAAm Beads, and Generation of Fluorescent Nitrogen-Doped Carbon Nanoparticles



Preparation of Palladium Nanoparticles Embedded CPAAm Beads. In a typical synthesis, 100 mg of PAAm beads cross-linked with [VIm-4VBC][Cl] (CPPAm) was mixed with aqueous K₂PdCl₄ (2 mL, 10 mM) and stirred vigorously for 3 days. Gradually, the suspension of polymer beads developed dark brown color, indicating the formation of Pd NPs inside the beads (shown in Scheme 2). Finally, Pd NPs embedded polymer particles (Pd@CPAAM) were centrifuged from the

suspension for further analysis. A similar test was also performed using aqueous solution of [VIm-4VBC][Cl] as control experiment.

Preparation of Nitrogen-Doped Carbon (NC) and Pd NPs Loaded Carbon (Pd@NC) Nanoparticles. CPAAm polymer beads were carbonized to nitrogen-doped carbon nanoparticles following the process represented in Scheme 2. Typically, ~100 mg of dried and crushed beads was loaded into an alumina crucible, placed in a tube furnace. The sample was heated to 350 °C (at 1 °C/min) and maintained for 2 h under an Ar atmosphere. Afterward, the furnace was slowly cooled to room temperature to collect sooty black product. Additionally, palladium loaded carbon nanoparticle (Pd@NC NPs) was prepared from Pd@CPAAM nanoconjugate by the similar carbonization procedure.

Characterization. NMR Study. The ¹H NMR spectrum of the synthesized cross-linker [VIm-4VBC][Cl] was acquired in D₂O using a Bruker DPX 300 MHz spectrometer.

ESI Mass Spectrometry. The ESI mass spectrum of the as-synthesized cross-linker [VIm-4VBC][Cl] was recorded in a quadrupole time-of-flight (Q-TOF) Micro YA263 mass spectrometer.

Fourier Transform Infrared (FTIR) Spectroscopy. The spectra of the oven-dried CPAAm beads and carbon nanoparticles were recorded by mixing with KBr in a 1:100 (w/w) ratio using a PerkinElmer FTIR Spectrum-400 spectrometer.

Optical Microscopy (OM). The fluorescent microscopic images of CPAAm–Eosin B conjugate beads, NC NPs, were acquired in an Olympus optical microscope (Model BX51) equipped with an Olympus U-RFL-T at 100× magnification at two different wavelengths: 517 and 310 nm, respectively.

Dynamic Light Scattering (DLS) Measurement. DLS and zeta potential of the CPAAm beads were measured on a Malvern Zetasizer NANO ZS 90 (Model No. 3690) using a HeNe gas laser operating at a wavelength of 632.8 nm at 25 °C. Generally, ~2 mg of CPAAm beads was dispersed in 2 mL of distilled water and filtered through a membrane filter of 0.45 μm pore size before measurements.

Field Emission Scanning Electron Microscopy (FESEM). Properly dried CPAAm beads and carbon nanoparticles were redispersed in water, sonicated for 1 h, and then drop-casted onto a coverslip, which were then adhered on a copper tape, supported on a metal stub and sputter coated with platinum to minimize charging before acquiring images. FESEM images were then acquired by placing the sample under a ZEISS JSM-6700F electron microscope operating at an accelerating voltage of 5 kV.

Photoluminescence Study. Photoluminescence (PL) spectra of the dispersion of CPAAm–Eosin B conjugate and carbon nanoparticles were recorded using a Jobin-Yvon Fluoromax-3 spectrometer upon excitation at 517 and 300 nm, respectively, using a slit width of 5 nm.

X-ray Diffraction (XRD) Study. The diffractograms of properly dried powder samples of NC NPs were recorded by using a Bruker AXS D8 Advance diffractometer at an accelerating voltage of 40 kV using a Cu K α ($\lambda = 1.5405 \text{ \AA}$) as the radiation source with a current intensity of 40 mA.

Elemental Analysis. The elemental analysis of nitrogen-doped carbon nanoparticle was carried out using a PerkinElmer 2400 series II CHN analyzer.

Raman Spectroscopy. Raman spectra of carbon nanoparticles were obtained at room temperature by a triple Raman spectrometer (Model T64000) using a 514.5 nm Ar⁺ laser at a

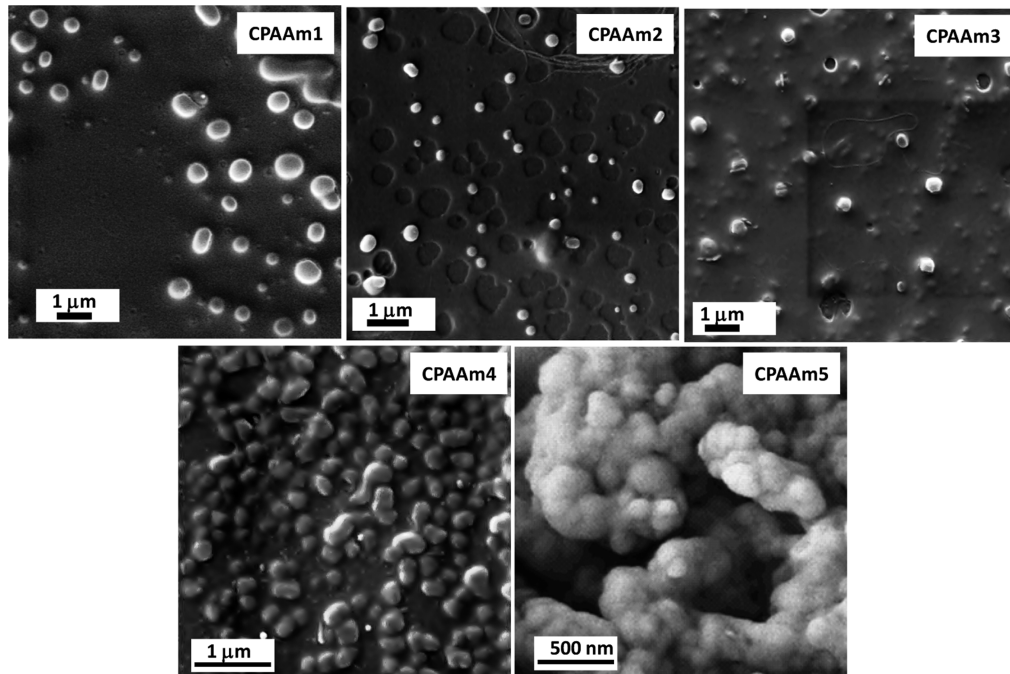


Figure 1. FESEM images of CPAAm nanobeads prepared by dispersion polymerization using different amount of IL cross-linker and PVME stabilizer.

power of 1 mW. All the spectra were normalized to the intensity of the G band for comparison. In the present work, we used the first- and second-order Raman spectra for examination of the effect of nitrogen doping on the structure of carbon nanoparticles.

Transmission Electron Microscopy (TEM). For a transmission electron microscopic study, one drop of aqueous dispersion of Pd@CPAAM conjugates, NC NPs, and Pd@NC NPs were placed on a carbon-coated Cu grid and allowed to dry in air. The grids were then observed on a JEOL JEM-2010 electron microscope operated at an accelerating voltage of 100 kV.

■ RESULTS AND DISCUSSION

Synthesis of the Ionic Liquid Cross-Linker-Based Cationic Poly(acrylamide) Beads. A new ionic liquid cross-linker [VIm-4VBC][Cl] was synthesized by coupling *N*-vinylimidazole with 4-vinylbenzyl chloride (see Scheme 1). The dried compound was a room temperature ionic liquid and water-soluble. The ¹H NMR spectrum (Figure S1 in the Supporting Information) showed the characteristic signals of ring protons of 4-vinylbenzyl chloride (δ 7.505 ppm), bridging methylene protons (δ 3.483 ppm), and ring protons of imidazolium cation (δ 10.194, 8.387, and 8.093 ppm). The ESI mass spectrum (Figure S2 in the Supporting Information) of the IL cross-linker showed the presence of only two sharp peaks: one at m/z 211 corresponding to the cationic part of the as-synthesized IL cross-linker and the other at m/z 117 for 4-vinylbenzyl cation (formed due to the fragmentation of the ionic liquid under high-energy irradiation). The absence of other peaks in the mass spectrum indicated that the ionic liquid was free from impurities of the starting materials.

Afterward, we employed this IL as a cross-linker for dispersion polymerization of acrylamide in the presence of APS as radical initiator and PVME as stabilizer in water/*tert*-butanol (1:1) mixed solvent. Typically, the concentration of

PVME with respect to the total solution was 2 wt %, and the amount of cross-linker with respect to the monomer was 5%. The synthesized CPAAm nanobeads were easily redispersible in water as shown in Scheme 2. However, the aqueous dispersion of CPAAm nanobeads were stable for 4–5 h. Several different concentrations of PVME and IL cross-linker were varied keeping other conditions same to prepare different beads (CPAAM1, CPAAM2, CPAAM3, CPAAM4, and CPAAM5) of varying sizes (see Table 1). FESEM images of the obtained CPAAM beads prepared with the variation of cross-linker and PVME concentrations were acquired and were presented in Figure 1. The beads were spherical in shape with sizes ranging from 147 to 480 nm depending on the concentrations of cross-linker and stabilizer PVME used in the reactions (see Table 1). As can be seen from Table 1, the size of the CPAAM bead decreased from 480 to 242 nm on increasing concentration of the stabilizer from 1 to 4 wt %, respectively, for CPAAM1 to CPAAM3, respectively, as was also reported earlier by Ray et al. without using any cross-linker.¹² Increase of the stabilizer concentration results in the faster surface adsorption on the growing polymer beads, which leads to decrease in the particle size. We also studied the effect of increase of the percentage of ionic liquid cross-linker from 2.5% to 10%, which resulted in the decrease of CPAAM bead size from 336 to 147 nm, respectively, for CPAAM4 and CPAAM5 samples, respectively, due to shrinkage of particles by internal network structures (see Table 1). However, CPAAM4 beads were not of well-defined shapes unlike other CPAAM samples. This observation might be due to low cross-linking density in CPAAM4 beads which produced irregular shapes. Again, CPAAM5 beads were highly aggregated. We believe a very high cross-linking density caused higher degree of shrinking and produced smaller sized but aggregated CPAAM nanobeads with respect to other samples. In this case, interestingly CPAAM2 samples exhibited minimum polydispersity index of around 0.98 owing to use of optimum combinations of stabilizer and cross-linker molecules during

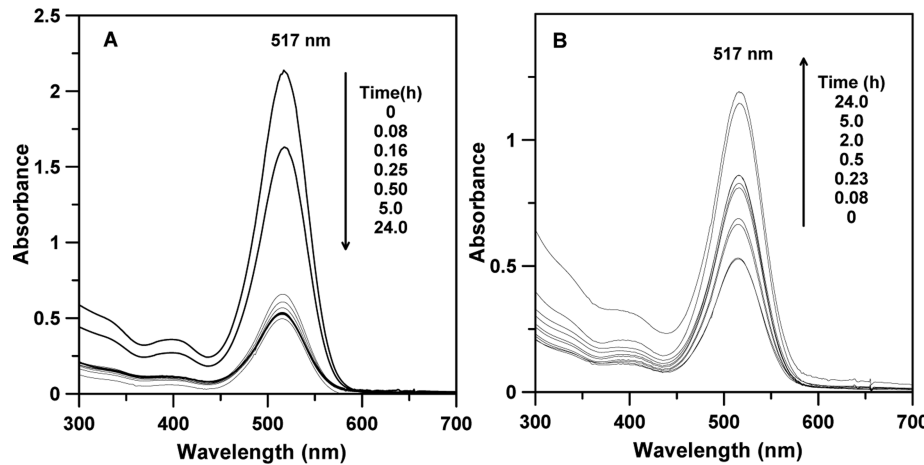


Figure 2. Successive UV–vis absorption spectra of Eosin B present in the supernatant solution during (A) dye adsorption and (B) dye release by cationic CPAAm beads.

dispersion polymerization. Additionally, the distribution of hydrodynamic sizes of CPAAm beads (represented in Figure S3) was investigated via DLS measurements which were found to be little bit higher than that obtained from FESEM study, but in good correlation in all cases. We have also measured the zeta potential of different CPAAm beads, such as CPAAm₂, CPAAm₄, and CPAAm₅, where the mol % of cross-linker was varied. It is expected that the polymer beads should not have high zeta potential value as observed for inorganic nanoparticle. However, the presence of ionic liquid cross-linker may have an effect in its zeta potential values due to the mobility of unbound anion of ionic liquid cross-linker on the surface of the bead. It was observed that the zeta potential value gradually increased with the increase of the mol % of IL cross-linker (see Figure S4 in the Supporting Information). For CPAAm₄ sample the value was negative, suggesting the adsorption of water on the surface. Alternatively, for CPAAm₂ and CPAAm₅ samples, the value rises, which means variation of mol % of ionic segment in the polymer bead tunes its surface charge, which is not yet reported. However, the reason for low positive zeta potential values of various aqueous dispersions of CPAAm beads is obviously due to the presence of very few fractions of cross-linking moieties in the vicinity of the surface.

The FTIR spectrum of the properly dried CPAAm₂ beads (prepared with 2 wt % of PVME and 5% cross-linker) showed broad bands at 3325 and 3157 cm⁻¹ for –NH stretching of amide and aromatic –CH– of imidazolium group and sharp bands at 1660 and 1560 cm⁻¹ for amide I and amide II, respectively, as shown in Figure S5 of the Supporting Information. Additionally, the methylene symmetric and asymmetric stretching bands at 2850 and 2922 cm⁻¹ confirmed conversion of –CH=CH₂ (vinyl unit of monomer) to >CH–CH₂–, i.e., indicating successful polymerization.

Study of Dye Exchange of Cationic CPAAm Beads. The presence of IL cross-linker makes CPAAm bead a polycationic network with mobile anions (see Scheme 1). Thus, the anion exchange ability of the as-synthesized cationic CPAAm₂ beads was studied using Eosin B, an anionic dye (see the Experimental Details section), and the exchange capacity was monitored by UV–vis spectroscopy. A gradual decrease in absorbance of Eosin B at 517 nm of the supernatant solution was observed with time after removal of the dye conjugated polymer bead (CPAAm–Eosin B) by centrifugation (Figure 2A). The calculation revealed that ~76% of dye was absorbed

by the CPAAm nanobeads on reaching equilibrium after 24 h (inset of Figure S6A). This corresponds to the binding of 1.6331 mmol of Eosin B per gram of the CPAAm nanobeads. When sodium acetate salt solution was added to this dispersion of equilibrated CPAAm–Eosin B conjugate, dye release was observed, which was studied by monitoring the gradual increase in absorbance of Eosin B with time in the supernatant solution obtained after centrifugation of the CPAAm–Eosin B conjugate bead (Figure 2B). Almost 56% of the adsorbed dye was released and 44% was retained in the CPAAm after 24 h (Figure 2B).

This study revealed that the anionic dye replaced the mobile Cl⁻ of the bead to produce CPAAm–Eosin B conjugate. Further, the dye was replaced by OAc⁻ ion of NaOAc. Further, the role of ionic cross-linker in the interaction between the dye molecules and polymer beads was explored by photoluminescence study. The fluorescence emission spectra showed a shift in emission maximum from 542 nm (for neat Eosin B) to 583 nm (for CPAAm–Eosin B conjugate) and 600 nm (for [VIm-4VBC][Eosin B] salt) (Figure S6A). Fluorescence light microscopic image of CPAAm–Eosin B conjugate showed red light emitting beads and thus further confirmed the successful exchange of Eosin B with cross-linked polymer nanobeads without any distortion of spherical shape of initial CPAAm nanobeads (Figure S6B). However, it is apparent from the optical microscopic image that most of the CPAAm–Eosin B conjugated particles are in the size range of micrometers. Actually, these are aggregated dye adsorbed polymeric nanoparticles. A similar test was also performed with Crystal violet (cationic dye), where no adsorption of dye by the cationic CPAAm beads were observed because of strong repulsion between the like charges.

Preparation of Pd NPs Loaded CPAAm (Pd@CPAAm) Conjugate Nanobeads. As cationic CPAAm beads could effectively and selectively bind with anions, so we tried to generate Pd NPs inside the CPAAm bead through the incorporation of PdCl₄²⁻ anion to CPAAm by anion exchange and subsequent reduction. The objective was to make CPAAm bead a precursor as well as template for Pd NPs. Unexpectedly, during anion exchange, a dark brown color was developed, revealing the *in situ* reduction of Pd(II) to Pd(0) by the ionic segment of the polymer beads (see Scheme 2) as described below. The TEM investigation shown in Figure 3A suggested that the Pd NPs were generated inside CPAAm beads. The

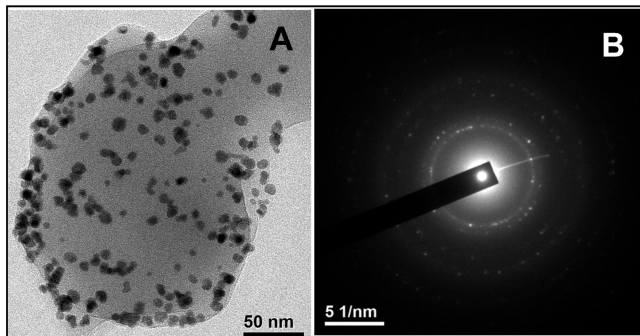


Figure 3. (A) TEM image and (B) SAED pattern of Pd@CPAAm nanoparticles.

average diameters of the spherical Pd NPs were measured to be around 7.5 nm. They were generated mostly beneath the surface of the CPAAm beads. The SAED pattern (Figure 3B) confirmed the fcc lattice structure of polycrystalline Pd NPs. The EDX mapping showed the signals of Pd in the sample (Figure S7). The exact reason for the CPAAm to act as a reducing agent for palladium salts is ambiguous. However, Gao et al. reported that imidazolium cation itself can act as a reducing agent to yield prismatic gold nanoparticles, as the extended hydrogen-bonding interaction of AuCl_4^- and imidazolium ring help to generate Au(0).⁶¹ To address this issue in our case, we have mixed the neat [VIm-4VBC][Cl] IL with the K_2PdCl_4 in water. We observed gradual brown coloration of the solution due to the formation of Pd(0). The TEM image given in Figure S8 of the Supporting Information clearly displayed the formation of spherical Pd NPs generated from the [VIm-4VBC][Cl] itself. However, the particles are of comparatively bigger in size (~ 100 nm) and a bit aggregated in nature, which is obvious due to absence of any stabilizing agent. Therefore, we can conclude that imidazolium cation present in the CPAAm beads actually act as a reductant-cum-template to produce Pd NPs loaded CPAAm nanobeads.

Synthesis of Nitrogen-Doped Carbon Nanoparticle (NC NPs) from CPAAm and Their Characterization. As it is well-known that cross-linking plays a vital role in the development of rigid structure,⁶² we extended the idea to prepare nitrogen-doped carbon from CPAAm by anaerobic carbonization of CPAAm2 at 350 °C. This produced fine powdery carbon nanoparticles, which can be easily redispersed in water (shown in Scheme 2). A typical FTIR spectrum of carbonized nanoparticles (Figure S5 in the Supporting Information) exhibited a N–H stretching band at ~ 3200 – 3400 cm^{-1} , a C–N stretching band at $\sim 1226 \text{ cm}^{-1}$, and a C≡N stretching band at $\sim 1570 \text{ cm}^{-1}$, confirming nitrogen doping of carbon structures.⁶³ The C, H, and N data of the carbon samples (carbon: 46.5%; hydrogen: 2.8%; nitrogen: 13.6%) clearly revealed that were highly doped with nitrogen. Raman signature peaks for pseudo graphitic carbon nanostructures were observed at 1359, 1587 and 2810 cm^{-1} corresponding to D, G and G' bands respectively (see Figure S9 in the Supporting Information).⁶⁴ The wide-angle XRD pattern of NC NPs showed an intense reflection peak at $2\theta = 26.17^\circ$ and a broad hump at $2\theta = 44.2^\circ$ (Figure S10 in the Supporting Information) corresponding to (002) and a superposition of (100) and (101) planes, respectively, from the pseudo-graphitic structure of NC NPs.^{48,65} These two reflection peaks were rather broad, indicating disordered but mainly contained sp^2 -hybridized carbon.¹⁵ FESEM study showed that NC NPs well

replicated the morphology and size of the CPAAm beads with little bit aggregation (Figure 4A). The average particle size of

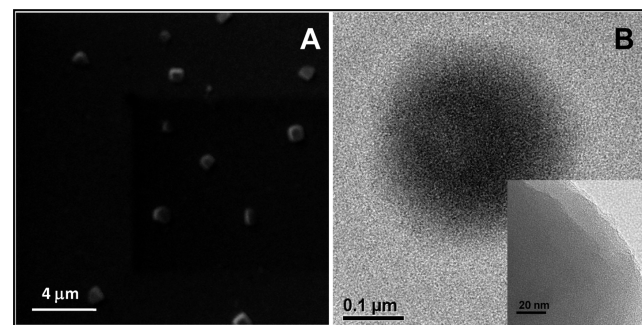


Figure 4. (A) FESEM and (B) HRTEM images of NC nanoparticles.

the NC NPs as calculated from FESEM was found to be 269 nm. The TEM image (Figure 4B) and HRTEM image (Figure 4B, inset) displayed roughly spherical NC NPs.

The aqueous dispersion of NC NPs had faint purple appearance (as shown in Scheme 2). Thus, we examined the UV-vis spectra of the carbon sample in its aqueous dispersion (Figure S11). However, it did not show any characteristic peak within the UV-vis region (300–900 nm). Nevertheless, it exhibited strong blue fluorescence when irradiated with UV lamp at 254 nm (Scheme 2). The fluorescence emission spectrum of aqueous dispersion of NC NPs revealed an emission maximum at 390 nm with intensity in the order of 10^6 cps when excited at 300 nm (Figure 5A). Finally, strong blue

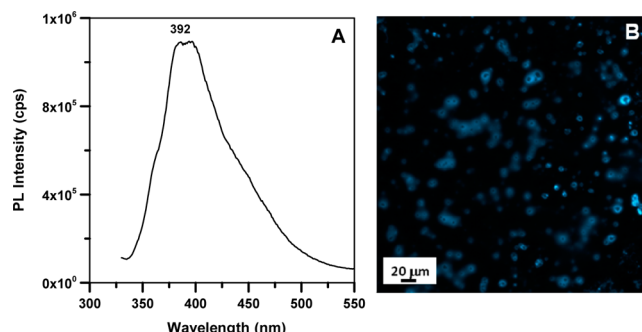


Figure 5. (A) Emission spectrum of aqueous dispersion of NC NPs and (B) fluorescent microscopic image of NC NPs.

light emitting dots were observed when viewed under fluorescent microscope (Figure 5B). However, NC NPs were very much aggregated and thus appeared to be of micron size in optical microscopic image. Generally carbon nanoparticles less than 10 nm exhibits strong blue fluorescence, while carbon particles in the range of 300 nm have either no or very weak fluorescence property.⁶⁶ However, in this case, the as-prepared carbon nanostructure with the diameter of 269 nm exhibits fluorescence property due to nitrogen doping. In this case, the presence of nitrogen defect in the carbon nanostructures are probably the reason for strong blue fluorescence which is similar to the report of Liu et al. where nitric acid-treated carbon soot exhibits strong fluorescence under UV excitation.⁶⁷

Preparation and Characterization of Pd NPs Embedded Nitrogen-Doped Carbon (Pd@NC) Nanoparticles. Carbon nanoparticle is an inert support and highly active material which give easy access of adsorbed molecules to the

catalytic sites housed inside the carbon. As discussed above, palladium nanoparticles loaded CPAAm beads were prepared easily in one step. In addition to this, we were also successful to pyrolyze the CPAAm beads to fluorescent carbon nanoparticles. These encouraged us to prepare Pd NPs loaded carbon nanoparticle (Pd@NC) from Pd@CPAAm nanobeads. Typically, properly dried Pd@CPAAm beads were carbonized at 350 °C at the heating rate of 1 °C/min for 2 h under a blanket of argon gas. When sufficiently cooled, the carbonized mass of Pd@NC NPs was ground to fine black powders. TEM image of the Pd NPs loaded carbon revealed that Pd NPs were generated and were uniformly distributed throughout the carbon nanoparticles matrix (Figure 6). Further, we have

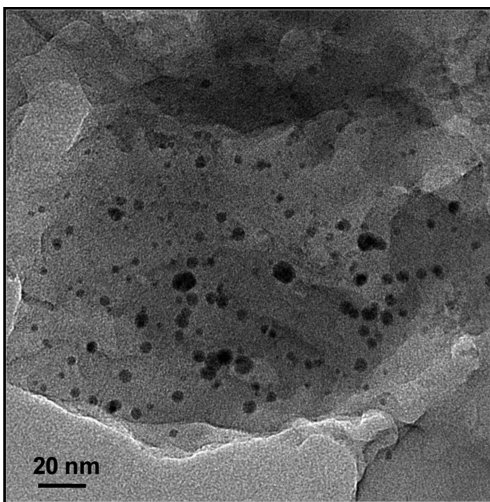


Figure 6. TEM image of one portion of Pd@NC nanoparticles.

studied its PL spectra (shown in Figure S12), which exhibit little decrease in the fluorescence intensity, compared to NC NPs. No doubt this Pd@NC NPs complex could be used as potential supported catalyst in various organic cross-coupling reactions, as reported by another group.⁶⁸

CONCLUSION

In the present work, we have designed a new imidazolium-based ionic liquid, which was subsequently utilized as ionic cross-linker for successful preparation of cross-linked poly(acrylamide) (CPAAm) nanobeads via dispersion polymerization using PVME as stabilizer. The nanobeads are redispersible in water, and their size can be tuned with simple variation of concentration of cross-linker and surface stabilizing polymer. Moreover, the CPAAm beads were cationic in nature due to the presence of imidazolium cation, which made them suitable for anion exchange. The anionic dye Eosin B was successfully exchanged with the mobile anion present inside CPAAm beads. Consecutively, the dye was released on addition of a pinch of sodium acetate. The reversible anion exchange was monitored spectrometrically, and that is useful for dye delivery purposes. The similar anion exchange with K₂PdCl₄ produced Pd NPs embedded polymer beads (Pd@CPAAm) owing to the presence of imidazolium cation in CPAAm beads which can simultaneously act as reductant and template. On the other hand, these CPAAm beads can be directly transformed into nitrogen-doped carbon nanoparticles by anaerobic carbonization at 350 °C, without the assistance of hard inorganic templates or highly cross-linked polymeric organic templates.

Not only the carbon nanoparticles nearly replicated the shape and size of the CPAAm beads, it also exhibited strong blue fluorescence when irradiated with UV light. This nitrogen-doped fluorescent carbon nanoparticles can be used as an imaging probe. Simultaneously, Pd@CPAAm nanobeads are also pyrolyzed to prepare palladium nanoparticles embedded carbon nanoparticles, which has strong potential to serve as good supported catalyst.

ASSOCIATED CONTENT

Supporting Information

¹H NMR and ESI-MS of [VIm-4VBC][Cl], FTIR and zeta potential data of CPAAm beads, TEM of Pd NPs, XRD, Raman spectra of carbon nanoparticles. This material is available free of charge via the Internet at <http://pubs.acs.org>.

AUTHOR INFORMATION

Corresponding Author

*Fax +91-33-24732805; e-mail psutkm@iacs.res.in (T.K.M.).

Author Contributions

T.D. and T.K.P. contributed equally to this manuscript.

Notes

The authors declare no competing financial interest.

ACKNOWLEDGMENTS

T.D. thanks the UGC, Government of India, for providing financial assistance. This research is supported by the grants from CSIR, New Delhi, India, and BRNS, Govt. of India.

REFERENCES

- (1) Rolland, A.; Wagner, N.; Chatelus, A.; Shroot, B.; Schaefer, H. Site-Specific Drug Delivery to Pilosebaceous Structures Using Polymeric Microspheres. *Pharm. Res.* **1993**, *10*, 1738–1744.
- (2) Davis, S. S.; Illum, L. Polymeric Microspheres as Drug Carriers. *Biomaterials* **1988**, *9*, 111–115.
- (3) Ober, C. K.; Lok, K. P.; Hair, M. L. Monodispersed, Micron-Sized Polystyrene Particles by Dispersion Polymerization. *J. Polym. Sci., Polym. Lett. Ed.* **1985**, *23*, 103–108.
- (4) Ugelstad, J.; Mfutakamba, H. R.; Mørk, P. C.; Ellingsen, T.; Berge, A.; Schmid, R.; Holm, L.; Jørgedal, A.; Hansen, F. K.; Nustad, K. Preparation and Application of Monodisperse Polymer Particles. *J. Polym. Sci., Polym. Symp.* **1985**, *72*, 225–240.
- (5) Lok, K. P.; Ober, C. K. Particle Size Control in Dispersion Polymerization of Polystyrene. *Can. J. Chem.* **1985**, *63*, 209–216.
- (6) Zhang, J.; Zhang, W.; Wang, Y.; Zhang, M. Palladium-Imidodiacetic Acid Immobilized on Ph-Responsive Polymeric Microspheres: Efficient Quasi-Homogeneous Catalyst for Suzuki and Heck Reactions in Aqueous Solution. *Adv. Synth. Catal.* **2008**, *350*, 2065–2076.
- (7) Szabo, T.; Molnar-Nagy, L.; Bognar, J.; Nyikos, L.; Teleghi, J. Self-Healing Microcapsules and Slow Release Microspheres in Paints. *Prog. Org. Coat.* **2011**, *72*, 52–57.
- (8) Zou, Y.; Zhang, Y. H.; He, P. X. Synthesis and Characterization of Amphoteric Polyacrylamide by Dispersion Polymerization in Aqueous Salts Solution. *Des. Monomers Polym.* **2013**, *16*, 592–600.
- (9) Lee, K.-C.; Lee, S.-E.; Choi, Y.-J.; Song, B.-K. Dispersion Polymerization of Acrylamide Int-Butyl Alcohol/Water Media. *Macromol. Res.* **2004**, *12*, 213–218.
- (10) Yuan, J.; Antonietti, M. Poly(Ionic Liquid) Latexes Prepared by Dispersion Polymerization of Ionic Liquid Monomers. *Macromolecules* **2011**, *44*, 744–750.
- (11) Klein, S. M.; Manoharan, V. N.; Pine, D. J.; Lange, F. F. Preparation of Monodisperse PMMA Microspheres in Nonpolar Solvents by Dispersion Polymerization with a Macromonomeric Stabilizer. *Colloid Polym. Sci.* **2003**, *282*, 7–13.

- (12) Ray, B.; Mandal, B. M. Dispersion Polymerization of Acrylamide: Part II. 2,2'-Azobisisobutyronitrile Initiator. *J. Polym. Sci., Part A: Polym. Chem.* **1999**, *37*, 493–499.
- (13) Li, F.; Geng, C.; Yan, Q. Growth Kinetics of Monodisperse Polystyrene Microspheres Prepared by Dispersion Polymerization. *J. Polym.* **2013**, *2013*, 7.
- (14) Jiang, Z. Z.; Zhu, J. R. Cationic Polyacrylamide: Synthesis and Application in Sludge Dewatering Treatment. *Asian J. Chem.* **2014**, *26*, 629–633.
- (15) Yuan, J.; Giordano, C.; Antonietti, M. Ionic Liquid Monomers and Polymers as Precursors of Highly Conductive, Mesoporous, Graphitic Carbon Nanostructures. *Chem. Mater.* **2010**, *22*, 5003–5012.
- (16) Yuan, J.; Marquez, A. G.; Reinacher, J.; Giordano, C.; Janek, J.; Antonietti, M. Nitrogen-Doped Carbon Fibers and Membranes by Carbonization of Electrospun Poly(ionic liquid)s. *Polym. Chem.* **2011**, *2*, 1654–1657.
- (17) Maka, H.; Spychar, T.; Pilawka, R. Epoxy Resin/Ionic Liquid Systems: The Influence of Imidazolium Cation Size and Anion Type on Reactivity and Thermomechanical Properties. *Ind. Eng. Chem. Res.* **2012**, *51*, 5197–5206.
- (18) Rahmathullah, M. A. M.; Jeyarajasingam, A.; Merritt, B.; VanLandingham, M.; McKnight, S. H.; Palmese, G. R. Room Temperature Ionic Liquids as Thermally Latent Initiators for Polymerization of Epoxy Resins. *Macromolecules* **2009**, *42*, 3219–3221.
- (19) Soares, B. G.; Livi, S.; Duchet Rumeau, J.; Gerard, J. F. Synthesis and Characterization of Epoxy/MCDEA Networks Modified with Imidazolium-Based Ionic Liquids. *Macromol. Mater. Eng.* **2011**, *296*, 826–834.
- (20) Huang, Z.; Shu, X.; Ran, Q. P.; Liu, J. P. Synthesis and Characterization of Cationic Polyacrylamide Aqueous Dispersion. *Acta Polym. Sin.* **2013**, *31*, 1013–1019.
- (21) Biswas, K.; Rao, C. N. R. Use of Ionic Liquids in the Synthesis of Nanocrystals and Nanorods of Semiconducting Metal Chalcogenides. *Chem.—Eur. J.* **2007**, *13*, 6123–6129.
- (22) Kim, K. S.; Choi, S.; Cha, J. H.; Yeon, S. H.; Lee, H. Facile One-Pot Synthesis of Gold Nanoparticles Using Alcohol Ionic Liquids. *J. Mater. Chem.* **2006**, *16*, 1315–1317.
- (23) Dinda, E.; Si, S.; Kotal, A.; Mandal, T. K. Novel Ascorbic Acid Based Ionic Liquids for the in Situ Synthesis of Quasi-Spherical and Anisotropic Gold Nanostructures in Aqueous Medium. *Chem.—Eur. J.* **2008**, *14*, 5528–5537.
- (24) Precht, M. H. G.; Campbell, P. S.; Scholten, J. D.; Fraser, G. B.; Machado, G.; Santini, C. C.; Dupont, J.; Chauvin, Y. Imidazolium Ionic Liquids as Promoters and Stabilizing Agents for the Preparation of Metal(0) Nanoparticles by Reduction and Decomposition of Organometallic Complexes. *Nanoscale* **2010**, *2*, 2601–2606.
- (25) Thiot, C.; Schmutz, M.; Wagner, A.; Mioskowski, C. Polyionic Gels: Efficient Heterogeneous Media for Metal Scavenging and Catalysis. *Angew. Chem., Int. Ed.* **2006**, *45*, 2868–2871.
- (26) Yoon, S.; Lee, J.; Hyeon, T.; Oh, S. M. Electric Double Layer Capacitor Performance of a New Mesoporous Carbon. *J. Electrochem. Soc.* **2000**, *147*, 2507–2512.
- (27) Vinu, A.; Hossain, K. Z.; Kumar, G. S.; Ariga, K. *Carbon* **2006**, *44*, 530–536.
- (28) Han, S.; Sohn, K.; Hyeon, T. Fabrication of New Nanoporous Carbons Through Silica Templates and Their Application to the Adsorption of Bulky Dyes. *Chem. Mater.* **2000**, *12*, 3337–3341.
- (29) Baikousi, M.; Daikopoulos, C.; Georgiou, Y.; Bourlinos, A.; ZboRil, R.; Deligiannakis, Y.; Karakassides, M. A. Novel Ordered Mesoporous Carbon with Innate Functionalities and Superior Heavy Metal Uptake. *J. Phys. Chem. C* **2013**, *117*, 16961–16971.
- (30) Zhuang, X.; Wan, Y.; Feng, C.; Shen, Y.; Zhao, D. Highly Efficient Adsorption of Bulky Dye Molecules in Wastewater on Ordered Mesoporous Carbons. *Chem. Mater.* **2009**, *21*, 706–716.
- (31) Jin, X.; Balasubramanian, V. V.; Selvan, S. T.; Sawant, D. P.; Chari, M. A.; Lu, G. Q.; Vinu, A. Highly Ordered Mesoporous Carbon Nitride Nanoparticles with High Nitrogen Content: A Metal-Free Basic Catalyst. *Angew. Chem., Int. Ed.* **2009**, *48*, 7884–7887.
- (32) Chen, X.; Jun, Y.-S.; Takanabe, K.; Maeda, K.; Domen, K.; Fu, X.; Antonietti, M.; Wang, X. Ordered Mesoporous Sba-15 Type Graphitic Carbon Nitride: A Semiconductor Host Structure for Photocatalytic Hydrogen Evolution with Visible Light. *Chem. Mater.* **2009**, *21*, 4093–4095.
- (33) Zhang, Y.; Wang, A.; Zhang, T. A New 3d Mesoporous Carbon Replicated from Commercial Silica as a Catalyst Support for Direct Conversion of Cellulose Into Ethylene Glycol. *Chem. Commun.* **2010**, *46*, 862–864.
- (34) Joo, S. H.; Choi, S. J.; Oh, I.; Kwak, J.; Liu, Z.; Terasaki, O.; Ryoo, R. Ordered Nanoporous Arrays of Carbon Supporting High Dispersions of Platinum Nanoparticles. *Nature* **2001**, *412*, 169–172.
- (35) Lee, E. Z.; Jun, Y. S.; Hong, W. H.; Thomas, A.; Jin, M. M. Cubic Mesoporous Graphitic Carbon(Iv) Nitride: An All-in-One Chemosensor for Selective Optical Sensing of Metal Ions. *Angew. Chem., Int. Ed.* **2010**, *49*, 9706–9710.
- (36) Lee, J.; Yoon, S.; Hyeon, T.; M. Oh, S.; Bum Kim, K. Synthesis of a New Mesoporous Carbon and Its Application to Electrochemical Double-Layer Capacitors. *Chem. Commun.* **1999**, 2177–2178.
- (37) Yang, Z.; Xia, Y.; Mokaya, R. Enhanced Hydrogen Storage Capacity of High Surface Area Zeolite-Like Carbon Materials. *J. Am. Chem. Soc.* **2007**, *129*, 1673–1679.
- (38) Wei, J.; Zhou, D.; Sun, Z.; Deng, Y.; Xia, Y.; Zhao, D. A Controllable Synthesis of Rich Nitrogen-Doped Ordered Mesoporous Carbon for CO₂ Capture and Supercapacitors. *Adv. Funct. Mater.* **2013**, *23*, 2322–2328.
- (39) Kyotani, T.; Nagai, T.; Inoue, S.; Tomita, A. Formation of New Type of Porous Carbon by Carbonization in Zeolite Nanochannels. *Chem. Mater.* **1997**, *9*, 609–615.
- (40) Johnson, S. A.; Brigham, E. S.; Ollivier, P. J.; Mallouk, T. E. Effect of Micropore Topology on the Structure and Properties of Zeolite Polymer Replicas. *Chem. Mater.* **1997**, *9*, 2448–2458.
- (41) Rodriguez-Mirasol, J.; Cordero, T.; Radovic, L. R.; Rodriguez, J. J. Structural and Textural Properties of Pyrolytic Carbon Formed within a Microporous Zeolite Template. *Chem. Mater.* **1998**, *10*, 550–558.
- (42) Knox, J. H.; Kaur, B.; Millward, G. R. Structure and Performance of Porous Graphitic Carbon in Liquid Chromatography. *J. Chromatogr. A* **1986**, *352*, 3–25.
- (43) Wu, C. G.; Bein, T. Conducting Carbon Wires in Ordered, Nanometer-Sized Channels. *Science* **1994**, *266*, 1013–1015.
- (44) Lu, A.; Kiefer, A.; Schmidt, W.; Schuth, F. Synthesis of Polyacrylonitrile-Based Ordered Mesoporous Carbon with Tunable Pore Structures. *Chem. Mater.* **2003**, *16*, 100–103.
- (45) Kruk, M.; Dufour, B.; Celer, E. B.; Kowalewski, T.; Jaroniec, M.; Matyjaszewski, K. Grafting Monodisperse Polymer Chains from Concave Surfaces of Ordered Mesoporous Silicas. *Macromolecules* **2008**, *41*, 8584–8591.
- (46) Ryoo, R.; Joo, S. H.; Jun, S. Synthesis of Highly Ordered Carbon Molecular Sieves Via Template-Mediated Structural Transformation. *J. Phys. Chem. B* **1999**, *103*, 7743–7746.
- (47) Hu, Y. S.; Adelhelm, P.; Smarsly, B. M.; Hore, S.; Antonietti, M.; Maier, J. Synthesis of Hierarchically Porous Carbon Monoliths with Highly Ordered Microstructure and Their Application in Rechargeable Lithium Batteries with High-Rate Capability. *Adv. Funct. Mater.* **2007**, *17*, 1873–1878.
- (48) Banerjee, S.; Paira, T. K.; Kotal, A.; Mandal, T. K. Surface-Confining Atom Transfer Radical Polymerization from Sacrificial Mesoporous Silica Nanospheres for Preparing Mesoporous Polymer/Carbon Nanospheres with Faithful Shape Replication: Functional Mesoporous Materials. *Adv. Funct. Mater.* **2012**, *22*, 4751–4762.
- (49) Wu, D.; et al. Nanoporous Polystyrene and Carbon Materials with Core-Shell Nanosphere-Interconnected Network Structure. *Macromolecules* **2011**, *44*, 5846–5849.
- (50) Han, S.; Hyeon, T. Simple Silica-Particle Template Synthesis of Mesoporous Carbons. *Chem. Commun.* **1999**, 1955–1956.
- (51) Chai, G. S.; Yoon, S. B.; Yu, J. S.; Choi, J. H.; Sung, Y. E. Ordered Porous Carbons with Tunable Pore Sizes as Catalyst

Supports in Direct Methanol Fuel Cell. *J. Phys. Chem. B* **2004**, *108*, 7074–7079.

(52) Gierszal, K. P.; Jaroniec, M. Carbons with Extremely Large Volume of Uniform Mesopores Synthesized by Carbonization of Phenolic Resin Film Formed on Colloidal Silica Template. *J. Am. Chem. Soc.* **2006**, *128*, 10026–10027.

(53) Morishita, T.; Tsumura, T.; Toyoda, M.; Przepiorski, J.; Morawski, A. W.; Konno, H.; Inagaki, M. A Review of the Control of Pore Structure in MgO-Templated Nanoporous Carbons. *Carbon* **2010**, *48*, 2690–2707.

(54) Tang, W.; Xie, J. A Novel Template Route for Synthesizing Mesoporous Carbon Materials. *Chem. Lett.* **2011**, *40*, 116–117.

(55) Liang, C.; Hong, K.; Guiochon, G. A.; Mays, J. W.; Dai, S. Synthesis of a Large-Scale Highly Ordered Porous Carbon Film by Self-Assembly of Block Copolymers. *Angew. Chem., Int. Ed.* **2004**, *43*, 5785–5789.

(56) Tanaka, S.; Nishiyama, N.; Egashira, Y.; Ueyama, K. Synthesis of Ordered Mesoporous Carbons with Channel Structure from an Organic-Organic Nanocomposite. *Chem. Commun.* **2005**, 2125–2127.

(57) Meng, Y.; et al. A Family of Highly Ordered Mesoporous Polymer Resin and Carbon Structures from Organic-Organic Self-Assembly. *Chem. Mater.* **2006**, *18*, 4447–4464.

(58) Liang, C.; Dai, S. Synthesis of Mesoporous Carbon Materials via Enhanced Hydrogen-Bonding Interaction. *J. Am. Chem. Soc.* **2006**, *128*, 5316–5317.

(59) Zhao, J.; Niu, W.; Zhang, L.; Cai, H.; Han, M.; Yuan, Y.; Majeed, S.; Anjum, S.; Xu, G. A Template-Free and Surfactant-Free Method for High-Yield Synthesis of Highly Monodisperse 3-Aminophenol-Formaldehyde Resin and Carbon Nano/Microspheres. *Macromolecules* **2013**, *46*, 140–145.

(60) Ray, B.; Mandal, B. M. Dispersion Polymerization of Acrylamide. *Langmuir* **1997**, *13*, 2191–2196.

(61) Gao, Y.; Voigt, A.; Zhou, M.; Sundmacher, K. Synthesis of Single-Crystal Gold Nano- and Microprisms Using a Solvent-Reductant-Template Ionic Liquid. *Eur. J. Inorg. Chem.* **2008**, *2008*, 3769–3775.

(62) Lee, J. S.; Wang, X.; Luo, H.; Dai, S. Fluidic Carbon Precursors for Formation of Functional Carbon under Ambient Pressure Based on Ionic Liquids. *Adv. Mater.* **2010**, *22*, 1004–1007.

(63) Chan, L. H.; Hong, K. H.; Xiao, D. Q.; Lin, T. C.; Lai, S. H.; Hsieh, W. J.; Shih, H. C. Resolution of the Binding Configuration in Nitrogen-Doped Carbon Nanotubes. *Phys. Rev. B* **2004**, *70*, 125408.

(64) Bulusheva, L. G.; Okotrub, A. V.; Kinloch, I. A.; Asanov, I. P.; Kurenya, A. G.; Kudashov, A. G.; Chen, X.; Song, H. Effect of Nitrogen Doping on Raman Spectra of Multi-Walled Carbon Nanotubes. *Phys. Status Solidi B* **2008**, *245*, 1971–1974.

(65) Yang, C. M.; Weidenthaler, C.; Spliethoff, B.; Mayanna, M.; Schuth, F. Facile Template Synthesis of Ordered Mesoporous Carbon with Polypyrrole as Carbon Precursor. *Chem. Mater.* **2005**, *17*, 355–358.

(66) Li, H.; He, X.; Kang, Z.; Huang, H.; Liu, Y.; Liu, J.; Lian, S.; Tsang, C. H. A.; Yang, X.; Lee, S.-T. Water-Soluble Fluorescent Carbon Quantum Dots and Photocatalyst Design. *Angew. Chem., Int. Ed.* **2010**, *49*, 4430–4434.

(67) Liu, H.; Ye, T.; Mao, C. Fluorescent Carbon Nanoparticles Derived from Candle Soot. *Angew. Chem., Int. Ed.* **2007**, *46*, 6473–6475.

(68) Jiang, B.; Song, S.; Wang, J.; Xie, Y.; Chu, W.; Li, H.; Xu, H.; Tian, C.; Fu, H. Nitrogen-Doped Graphene Supported Pd@PdO Core-Shell Clusters for C-C Coupling Reactions. *Nano Res.* **2014**, *1*–11.